

Shear Elasticity Probe for Soft Tissues with 1-D Transient Elastography

Laurent Sandrin, Mickaël Tanter, Jean-Luc Gennisson, Stefan Catheline, and Mathias Fink

Abstract—Important tissue parameters such as elasticity can be deduced from the study of the propagation of low frequency shear waves. A new method for measuring the shear velocity in soft tissues is presented in this paper. Unlike conventional transient elastography [1], [2] in which the ultrasonic transducer and the low frequency vibrator are two separated parts, the new method relies on a probe that associates the vibrator and the transducer, which is built on the axis of the vibrator. This setup is easy to use. The low frequency shear wave is driven by the transducer itself that acts as a piston while it is used in pulse echo mode to acquire ultrasonic lines. The results obtained with the new method are in good agreement with those obtained with the conventional one.

I. INTRODUCTION

MEASURING the viscoelastic properties of soft tissues is of great interest because tissue stiffness may be related to a pathological state. Palpation remains the most commonly used technique in a clinical setting. It relies on qualitative estimation of the low frequency (LF) stiffness of tissue. There is a need for a noninvasive and quantitative system that could be used to measure stiffness response of the tissue.

Little information on the viscoelastic parameters of soft tissues is obtained using ultrasound-based methods. Truong [3], [4] measured *ex vivo* shear velocity and attenuation in frog skeletal muscle. Krouskop *et al.* [5] developed a Doppler-based system for making noninvasive measurements of the elastic modulus of soft tissue *in vivo*. Sonoelasticity and later sonoelastography have been described [6]–[9] to image tissue stiffness. It consists of stimulating the tissue with a monochromatic mechanical vibration (10 to 1000 Hz) and of measuring the relative tissue motion with a color Doppler instrument. Yamakoshi *et al.* [10] used a similar approach to measure the LF vibration velocity in phantoms, in pig leg muscle, and *in vivo* in human liver. Static elastography was developed by Ophir *et al.* [11]–[13] who use a quasi-static compression applied to the tissue to produce an image (elastogram) that depicts the distribution of the estimated strain in the tissue. Muthupillai *et al.* [14] and Dutt *et al.* [15] studied the propagation of shear waves in gel-based phantoms and beef striated muscles using magnetic resonance elastography (MRE). Local displacements were estimated using a

modified gradient-echo imaging pulse sequence. Quantitative measurements enable estimation of local shear wave velocity, shear modulus, and dispersion. Levinson *et al.* [16] applied sonoelastography *in situ* to collect vibration propagation velocities as a function of load in the quadriceps muscle of 10 volunteers. Young's modulus values were derived from shear velocities.

In our laboratory, Catheline *et al.* [1], [2] emphasized the biases induced by diffraction in sonoelastography and sonoelasticity when shear waves are generated by a forced monochromatic vibration. They showed that the apparent shear velocity depends on frequency because the classical theory of a plane wave propagation in a linear viscoelastic medium does not apply. To avoid these biases, they proposed to use a pulsed excitation driven by a piston vibrating perpendicularly to the surface of a half-space viscoelastic medium. The axial component of the displacements induced by the transient shear wave is estimated with an ultrasonic transducer placed on the opposite side of the medium. Using a pulsed excitation, they showed that diffraction biases could be eliminated and that both shear elasticity and shear viscosity could be measured. This method is termed transient elastography. The work of Catheline *et al.* was extended by Sandrin *et al.* [17], [18] to the study of 2-D shear wave propagation. For this application, high frame rate is required. Therefore, an ultra-fast ultrasonic imaging electronic system that can produce up to 10,000 frames/s was developed. Acquisition times are considerably reduced compared with MRI or Doppler techniques, which allow for investigation of moving organs.

Transient elastography suffered from an important drawback: because it worked in transmit mode, access to both sides of the medium under investigation was needed. In this paper, we propose an improved system in which the pulsed LF vibration is given by the ultrasonic transducer itself. This system is termed the reflection mode. The main difficulty that arises in reflection mode concerns the ultrasound-based measurement of absolute displacements within the medium because the transducer itself is moving. In Section II, the transmit mode is presented and used to estimate the shear elasticity in a homogeneous tissue-equivalent phantom. The reflection mode is developed in Section III. Different solutions are carefully analyzed, and the results are compared with those obtained in transmit mode. Good agreement between both methods allows us to validate our new system. The so-called shear elasticity probe is applied to the *in vivo* measurement of bicep shear elasticity in Section IV.

Manuscript received February 23, 2001; accepted November 9, 2001. The authors are grateful to the AFM for supporting this work.

The authors are with Laboratoire Ondes et Acoustique, École Supérieure de Physique et Chimie Industrielles de la Ville de Paris, Université Denis Diderot, CNRS UMR 7587, 75231 Paris, Cedex 05, France (e-mail: laurent.sandrin@espci.fr).

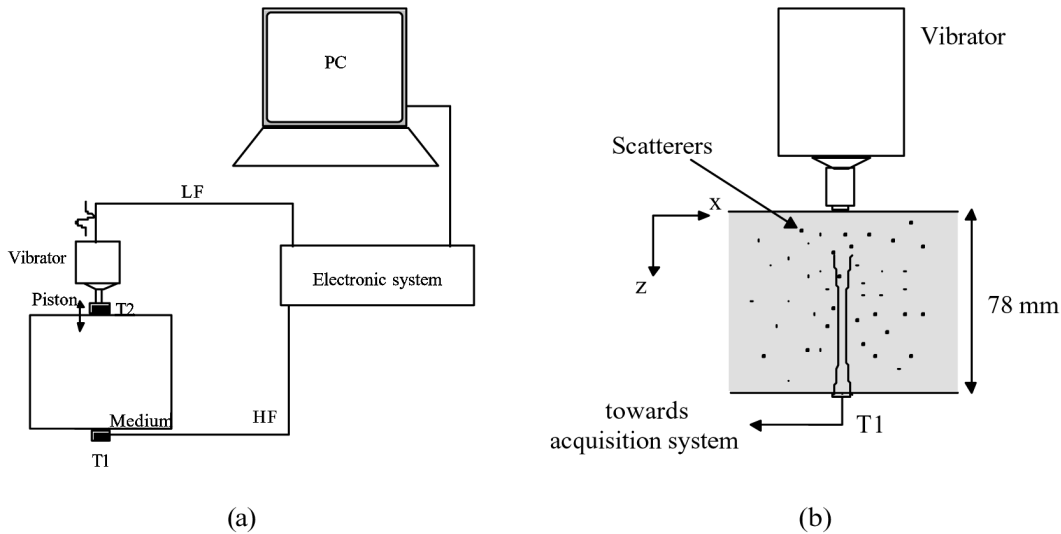


Fig. 1. Transmit mode experimental setup. T1 is placed on the opposite side of the medium.

II. TRANSMIT MODE

An isotropic linear elastic material can be described by two independent parameters such as the compressional modulus and the shear modulus. In soft tissues, the shear modulus is less than 1 MPa, and the compression modulus is on the order of 1 GPa [19]. Thus, at a fixed strain, shear displacements would be much larger than compressional displacements if shear and compression attenuations were identical. However, shear attenuation increases strongly with frequency. At ultrasonic frequencies, soft tissues behave similar to water because shear waves are fully attenuated. On the contrary, at LFs (less than 200 Hz), shear attenuation is low, and shear waves may be induced using an adapted LF vibrating device while compressional waves can be ignored. The transmit mode involves the propagation of both kinds of waves at different frequencies with highly different velocities. A shear wave is emitted with a LF vibration (50 Hz). It propagates slowly in soft tissues (1 to 10 m/s). The displacements induced in the medium by this wave are measured using a compression wave, an ultrasonic wave (5 MHz) propagating at about 1500 m/s.

A. Experimental Setup

The experimental setup is presented in Fig. 1. The entire system is operated with a personal computer (Pentium 300 MHz). An electronic system controls the LF excitation, and the ultrasonic pulsed echo mode. The LF excitation is obtained with a Brüel & Kjaer mini-shaker type 4810. The center frequency of the LF excitation typically ranges between 50 and 200 Hz. The shape and the frequency of the LF vibrations are arbitrary. Ultrasonic signals are sampled at 50 MHz. They are emitted and recorded using a 9-bit digitizer with 2 Mbytes of random access memory (RAM).

RF lines are usually acquired at a repetition frequency between 500 and 2000 Hz. The repetition frequency is only limited by the travel time of the ultrasonic pulse. In a 7.5-cm deep medium, where the speed of sound is 1500 m/s,

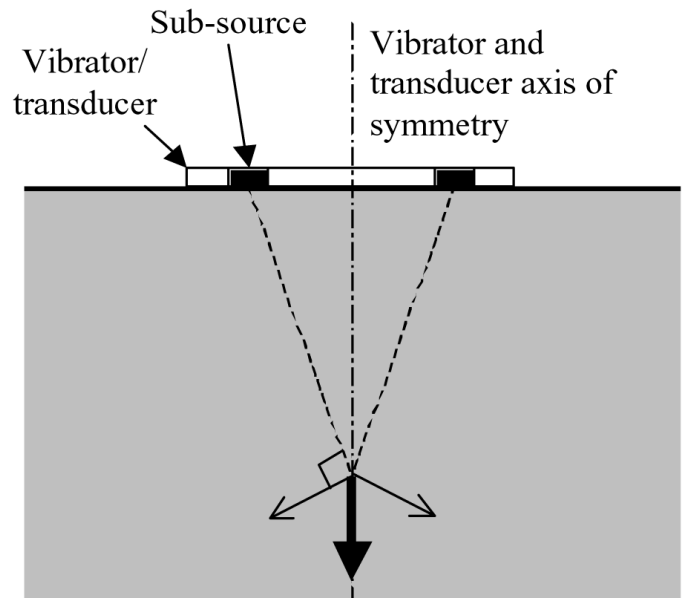


Fig. 2. Diffraction effects. The summed contributions of the transversely polarized shear waves coming from subsources give rise to a globally, longitudinally polarized shear wave on the axis of the vibrator.

the travel time of the ultrasound is $100 \mu\text{s}$, and, thus, the theoretical maximum acquisition rate is 10 000 RF lines/s. Because of the amount of RAM available (2 Mbytes), the number of RF lines that can be stored during an acquisition is limited (for example 400 RF lines for a 75-mm deep region of interest).

In this section, we study the transmit mode in which we use an ultrasonic transducer and a LF mini-shaker. As shown in Fig. 1, the ultrasonic transducer (T1) is placed on one side of the medium, and the mini-shaker vibrates on the opposite side, perpendicular to the surface. A second ultrasonic transducer (T2) is fixed to the axis of the mini-shaker and used as a piston-like vibrator (the displacement

of the vibrator is perpendicular to the piston surface) to induce the LF shear wave. T2 is not used to emit or receive ultrasonic signals. In Section III, T2 will be used both as a LF vibrator and as an ultrasonic transducer. Both ultrasonic transducers (T1 and T2) feature a diameter of 7.3 mm, a focal length of 34.5 mm, and a central frequency of 5.0 MHz.

The measurements have been performed in a tissue equivalent gel-based phantom. The phantom is homogeneous, and its size is $80 \times 150 \times 200$ mm. It is made with gelatin (4%) and agar (3%) powders mixed in hot water (80°C). 5% propanol-1 is added to the solution to increase the conservation duration. Agar powder is used as echogenic particles; gelatin concentration is related to elasticity.

B. Displacement Estimation

Different speckle tracking algorithms [11], [20] have been developed to estimate the axial or even lateral displacements or strains in soft tissue. In our study, speckle signals (RF lines) acquired with the electronic system are segmented versus depth z into 1-mm slices with 50% overlap. The axial displacement is estimated in each segment using the standard cross-correlation technique [11], [21] between successive RF lines that remain highly correlated because displacements are small. The precision is about $1 \mu\text{m}$ [22]. To increase the signal-to-noise ratio, RF lines and displacements are filtered using, respectively, a band-pass filter (2.5 to 7.5 MHz) and a low-pass filter (100 Hz).

Experimentally we measure the displacements along the ultrasonic axis that intercepts the vibrator. Actually, we have only access to the projection of the displacement vectors on the ultrasonic axis. Although, if the medium is invariant for any translation perpendicular to the ultrasonic axis, transverse displacements must be zero because of the cylindrical symmetry versus the vibrator-transducer axis. Furthermore, symmetry considerations also indicate that the shear and compression wave propagation directions are parallel to this axis. In conclusion, surprisingly, if there are displacements induced by the shear wave on the axis vibrator-transducer, they must be purely longitudinal. Although shear waves are purely transverse in the far field (where they can be considered as plane waves), they may have a longitudinal component in the near field of an extended source because of diffraction effects. As shown in Fig. 2, the summed contributions of the transversely polarized shear waves coming from sub-sources give rise to a globally longitudinally polarized shear wave on the axis of the vibrator.

Because the phantom is placed in a rectangular box, the cylindrical symmetry is valid until the shear wave reaches the edges.

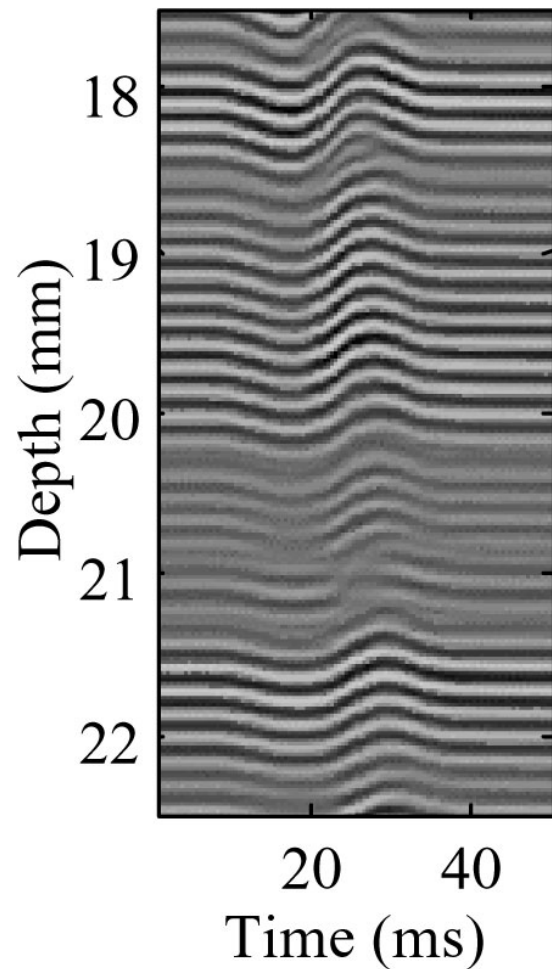


Fig. 3. Transmit mode. Part of the M-mode image composed of 100 RF lines stored while the LF shear wave propagates inside the medium.

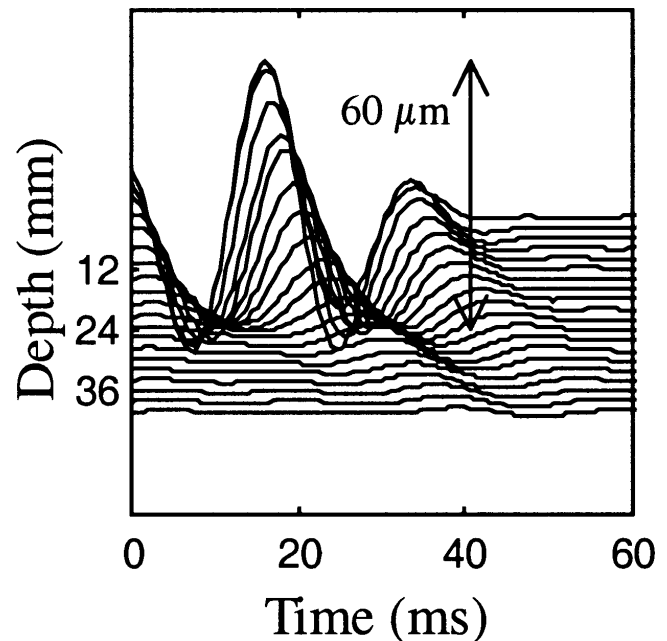


Fig. 4. Displacement estimates measured in the homogeneous phantom as a function of time and depth.

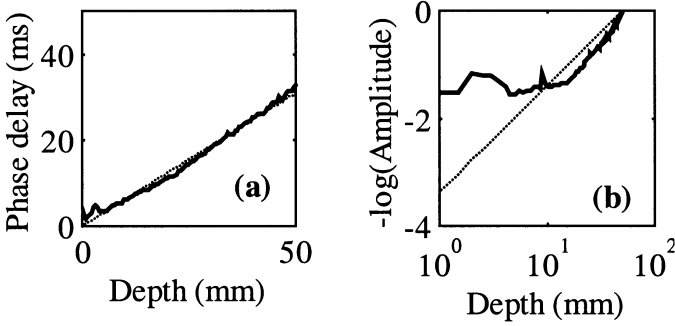


Fig. 5. Transmit mode. Phase delay (a) and amplitude (b) of the shear wave as a function of depth. A linear fit of the phase delay variation with depth (along the z direction) is performed between depths of 5 and 50 mm, indicating the shear phase velocity at 50 Hz, the value of which is 1.53 ± 0.03 m/s.

C. Elasticity Estimation

Elasticity in the medium is derived from the shear velocity. In an isotropic elastic medium, Young's modulus E and the Poisson ratio σ are expressed as

$$\begin{aligned} E &= \frac{\mu(3\lambda + \mu)}{\lambda + \mu} \\ \sigma &= \frac{\lambda}{2(\lambda + \mu)} \end{aligned} \quad (1)$$

where μ and λ are the Lamé coefficients, respectively, of the shear modulus and bulk modulus. These equations are valid in soft media if viscosity can be ignored. In soft media, $\lambda \gg \mu$ and, thus, E and σ simplify to

$$\begin{aligned} E &= 3\mu \\ \sigma &= \frac{1}{2}. \end{aligned} \quad (2)$$

The Young modulus only depends on the shear modulus. Because the shear modulus is small, the Poisson ratio is very close to $\frac{1}{2}$. It characterizes the quasi-incompressibility of the medium and indicates that shear waves will dominate within the medium. If the medium is purely elastic (dissipation can be ignored), the shear modulus satisfies [23]

$$\mu = \rho V_s^2 \quad (3)$$

where V_s is the shear velocity and ρ is the mass density. Consequently, given the shear velocity and mass density ρ , one easily deduces the Young's and shear moduli in a soft non-dissipative medium.

In our experiments, shear velocity is estimated using a linear regression of the phase versus depth variation at the center frequency of the LF vibration. Indeed, as long as diffraction effects and dissipation can be ignored, the phase velocity does not differ from the shear velocity [15].

D. Results

In the experiment, 100 RF lines are acquired with transducer T1 at a repetition frequency of 2000 RF lines/s during the shear wave propagation. The RF lines correspond

to a ROI between $Z = 5$ mm ($6.5 \mu\text{s}$) and $Z = 90$ mm ($117 \mu\text{s}$) on the axis of the vibrator. Part of the M-mode image composed of 100 RF lines between 17 and 23 mm is presented in Fig. 3. The total acquisition time is 50 ms. Shear wave is induced by sending a single cycle of a 50-Hz frequency sinusoid to the vibrator. The choice of a mean frequency of 50 Hz is a compromise between a lower frequency, which would lead to enhanced diffraction effects, and a higher frequency, which would be more attenuated in soft tissues. As explained by Catheline [15], diffraction effects induce biases in the velocity estimation.

Displacements estimated with the cross-correlation technique are presented in Fig. 4. The evolution of phase delay and amplitude of the shear wave are obtained using the angle and amplitude of the Fourier transform at the excitation central frequency (50 Hz). Results are shown in Fig. 5. The amplitude evolution versus depth [Fig. 5(b)] is complex. The amplitude remains approximately constant until 15 mm and decreases afterward as $1/z^2$, because the longitudinal displacements are dominated by a near-field term that decreases as $1/z^2$ as explained by Aki and Richards [24]. A linear fit of the phase delay evolution versus depth [Fig. 5(a)] is performed between depths of 5 and 50 mm. It indicates the shear phase velocity at 50 Hz, which value is 1.54 ± 0.02 m/s ($r^2 = 0.994$). Assuming that the density in the phantom is $1000 \text{ kg}\cdot\text{m}^{-3}$, the shear elasticity may be estimated from (3). It yields to a shear modulus of 2.36 ± 0.05 kPa. Thus, in the transmit mode, this technique allows an accurate estimation of the shear modulus with small error.

III. REFLECTION MODE

Because it requires access to both sides of the medium, the transmit mode is not convenient when access is limited. We developed a second mode termed reflection mode in which the transducer used to emit and receive ultrasonic signals also acts as a piston-like LF vibrator. In reflection mode, the measurement of absolute displacements within the medium is not direct because the transducer vibrates. The measured displacement of a tissue slice equals the absolute displacement induced by the shear wave minus the relative displacement of the transducer itself. Thus, we have to discriminate between the displacements because of the shear wave and those caused by the measurement device. The presence of a fixed interface echo in the RF lines provides a means to find the exact displacement of the vibrator and, thereafter, compensate the RF lines for its displacement. When no fixed interface echo can be found in the RF lines, an alternative solution is to assume that the shear wave attenuates sufficiently to neglect the displacement deep in the medium. It will be shown that such an assumption may induce biases in the shear velocity estimation if the assumption is not verified. Therefore, an ultimate solution based on strain estimation is proposed.

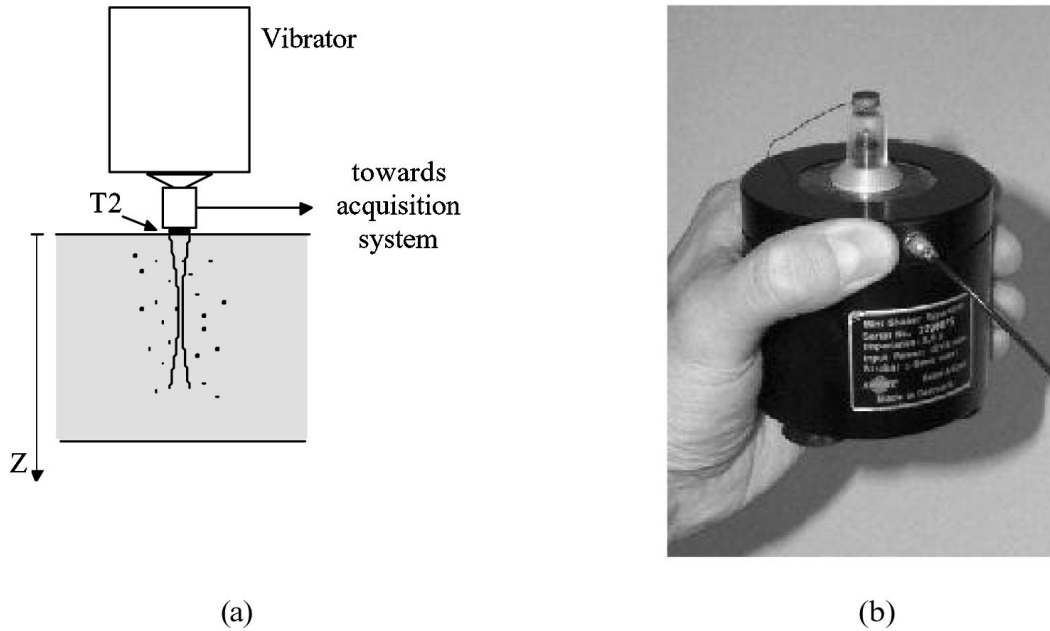


Fig. 6. a) Reflection mode experimental setup. T2 is fixed to the axis of the vibrator. b) The shear elasticity probe is composed of the vibrator and the transducer.

A. Transducer Relative Displacement Compensation

The experimental longitudinal displacements, $d(z,t)$, of tissue slices within the medium are measured relative to the transducer. When the transducer is motionless, as in transmit mode, the experimental displacements are the absolute displacements. On the other hand, when the transducer is used to generate the LF shear wave, the displacement of the transducer must be taken into account because the absolute displacements no longer equal the experimental displacements measured relative to the transducer. The exact displacement of the vibrator must be subtracted from those measurements to get the absolute displacements. The experimental displacements relative to the transducer are expressed as

$$d(z,t) = \delta(z,t) - D(t) \quad (4)$$

where z is the depth, $D(t)$ is the absolute displacement of the vibrator, and $\delta(z,t)$ is the absolute displacement at depth z caused by elastic wave propagation. The vibration is positioned at $z = 0$.

One finds several methods to eliminate $D(t)$ from (4). The simplest solution is to measure $d(z,t)$ and then take its derivative with respect to z , which eventually gives the strain. Unfortunately, with this method, the cross-correlation is noisier and time consuming because it requires the measurement of large displacements. Furthermore, derivation is very sensitive to noise.

The most promising method is to measure $D(t)$ instead of directly measuring $d(z,t)$. Once $D(t)$ is known, the RF lines can be shifted back to compensate for the vibrator displacement. Thereafter, displacements $\delta(z,t)$ are estimated using the cross-correlation technique applied to successive RF lines. The temporal shift is performed in the

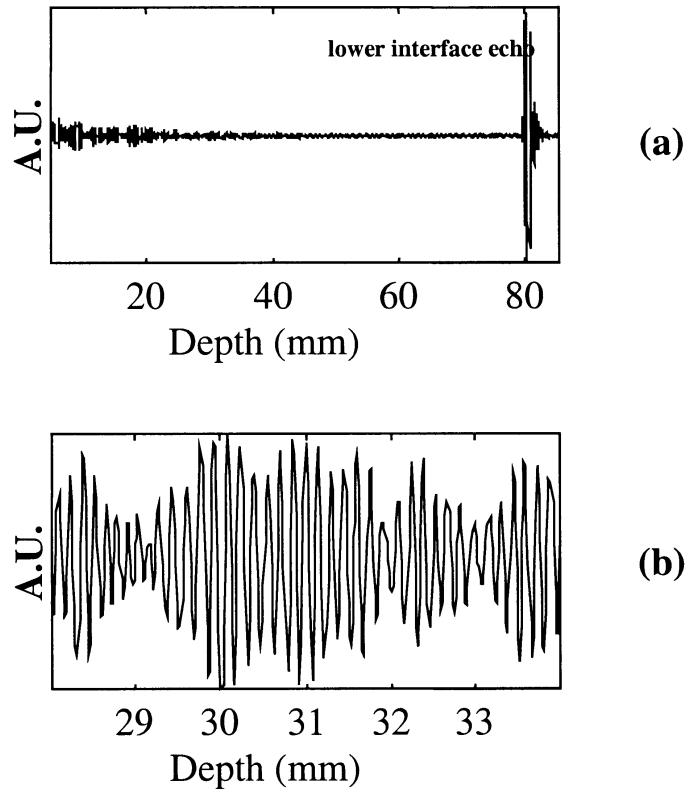


Fig. 7. Reflection mode. a) Echo signal (RF line) obtained in the phantom. The strong lower interface echo at 78 mm is clearly seen. b) Same signal between 25 and 35 mm (A.U. = arbitrary units).

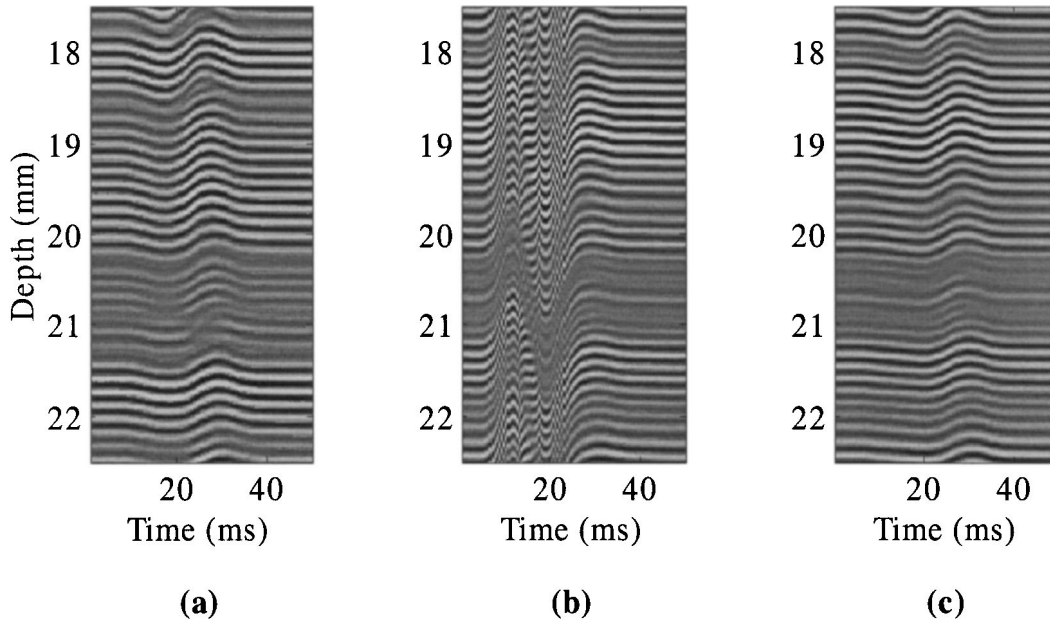


Fig. 8. Part of the M-mode image composed of 100 RF lines stored while the LF shear wave propagates inside the medium: a) in transmit mode, b) in reflection mode, and c) in reflection mode after compensation of the relative displacement of the vibrator.

Fourier domain. An RF line discrete Fourier transform is expressed as

$$R(k) = \sum_{n=0}^{N-1} r(n) \exp\left(-j\frac{2\pi nk}{N}\right) \quad (5)$$

where $r(n)$ is the sampled echo signal and N is the number of samples. If the RF line is acquired at time t_o , then the back-shifted RF line r_s is

$$r_s(n) = \sum_{k=0}^{N-1} R(k) \exp\left(j\frac{2\pi k}{N} \left(n + \frac{2D(t_o)}{cT_s}\right)\right) \quad (6)$$

where T_s is sampling period and c is speed of sound.

Vibrator displacement compensation is performed by estimating $D(t)$. In the following, we discuss the different techniques used in reflection mode to compensate the vibrator displacement and to correctly estimate shear velocity. The first technique consists of measuring a motionless interface relative displacement (MIRD). The relative displacement of the motionless object is, thus, exactly the opposite of $D(t)$. A second technique can be used when no motionless object echo is present. It consists of assuming that the elastic wave attenuation is sufficient for the displacements to be negligible at a certain depth in the medium. The vibrator displacement is deduced from the relative displacement of a deep echo. This technique is termed motionless deep echo assumption (MDEA). This second technique may lead to a biased estimation of the shear velocity if the attenuation of the elastic waves is not sufficient. However, one can take the derivative of the displacements versus depth, which yields to strain. Using the strain approach (SA), we show that the bias is removed. The derivation may be avoided by using an adap-

tive stretching technique [25]. The different techniques are compared with the transmit mode.

B. Results

In the reflection mode, transducer T2 is both used to acquire the RF lines and to act as a piston-like vibrator [Fig. 6(a)]. As shown in Fig. 6(b), the transducer is fixed to the axis of the mini-shaker. One hundred RF lines are acquired in the same conditions as in transmit mode. An RF line is presented in Fig. 7(a). The strong lower interface echo is clearly seen. Part of the M-mode image composed of 100 RF lines between 17 and 23 mm is presented in Fig. 8(b). This M-mode image must be compared with the one obtained in transmit mode presented in Fig. 8(a). For display consistency, RF lines are referred to the same coordinate system. As one can notice, the shift between successive RF lines is larger in Fig. 8(b) than in Fig. 8(a). The displacement of the vibrator induces large shifts in the RF lines that can be compensated using the following approaches.

1. *MIRD*: The exact displacement of the vibrator can be deduced from a MIRD. We used the echo of the lower interface of the medium at 78-mm depth as shown in Fig. 7(a). This movement is measured with a cross-correlation technique using a 2-mm window centered at 78-mm depth. The resulting displacement of the vibrator estimate is presented in Fig. 9(a). The cross-correlation coefficient between successive RF lines is very good; its inferior limit is 0.93 [Fig. 9(b)]. The amplitude of vibration is about 1 mm.

The relative displacement of the vibrator [Fig. 9(a)] can be used to shift back the RF lines. Fig. 8(c) presents the compensated RF lines that are close to those obtained in transmit mode [Fig. 8(a)]. After compensation, the

strong echo coming from the lower interface is motionless [Fig. 10(b)]. Thereafter, absolute displacements induced in the medium by the LF shear wave can be estimated [Fig. 11].

The evolutions of phase delay and amplitude of the shear wave as a function of depth are presented in Fig. 12. One notices that, in reflection mode, no information is obtained close to the vibrator. In fact, because T2 is both used as a transducer and as a LF vibrator, we are limited by the working region of the transducer itself. This implies that depths shallower than 5 mm are not investigated. The linear fit performed between a depth of 5 and 50 mm indicates a shear velocity estimate of 1.51 ± 0.02 m/s ($r^2 = 0.994$). Thus, the shear modulus is 2.28 ± 0.04 kPa.

2. *MDEA*: In the absence of motionless interface echo, another solution is to assume that the shear wave is sufficiently attenuated and that a late echo comes from a deep region inside the medium that hardly moves. Under such an assumption, the latest echo can be used to obtain the exact displacement of the vibrator using the cross-correlation technique with short length window.

The assumption of a motionless deep echo was tested for a depth of 50 mm with a 2-mm length window. The vibrator absolute displacement estimation is presented in Fig. 13(a). In contrast to the strong echo from the lower interface, we do not know if the echo at 50 mm comes from a motionless part of the medium. The error on the vibrator absolute displacement estimation is calculated by comparison with the exact vibrator absolute displacement obtained from the relative displacement of the motionless interface echo at 78 mm. The error is presented in Fig. 13(b). The error on the estimate of the vibrator displacement indicates that the medium experiences a displacement of $50 \mu\text{m}$ in amplitude at the depth of interest. Thus, the assumption of a motionless region of the medium is false. The error on the estimate of the displacement of the vibrator is maximum at 35 ms when the shear wave reaches this part of the medium. This error is not negligible compared with the displacement induced by the shear wave.

The displacement estimates obtained after compensation of the relative displacement of the transducer are presented in Fig. 14(a). The evolution of phase delay of the shear wave as a function of depth is presented in Fig. 14(b). The phase delay linear fit indicates a shear phase velocity at 50 Hz of 1.72 ± 0.04 m/s ($r^2 = 0.957$), which eventually gives a shear modulus of 2.96 ± 0.14 kPa.

3. *SA*: Strain estimates are obtained using a classical derivation algorithm (finite differences scheme with a five-point centered mesh) applied to the displacement estimates measured under MDEA mode. They are presented in Fig. 15(a). The evolution of phase delay of the shear wave as a function of depth is presented in Fig. 15(b). The phase delay linear fit indicates a shear phase velocity at 50 Hz of 1.54 ± 0.02 m/s ($r^2 = 0.996$). The shear modulus is 2.36 ± 0.04 kPa.

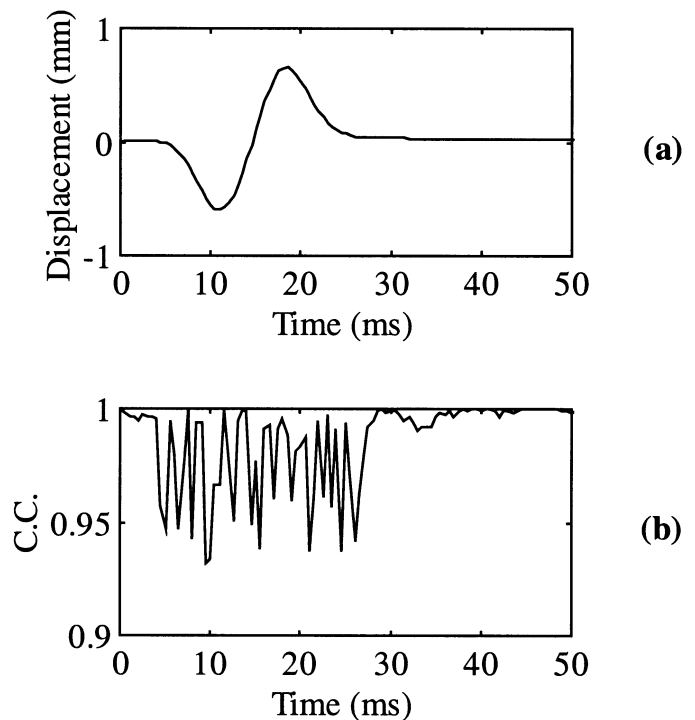


Fig. 9. a) Displacement estimates of the vibrator deduced from the relative displacement of the strong echo coming from the lower interface of the medium at $Z = 78$ mm and b) corresponding cross-correlation coefficient between successive RF lines.

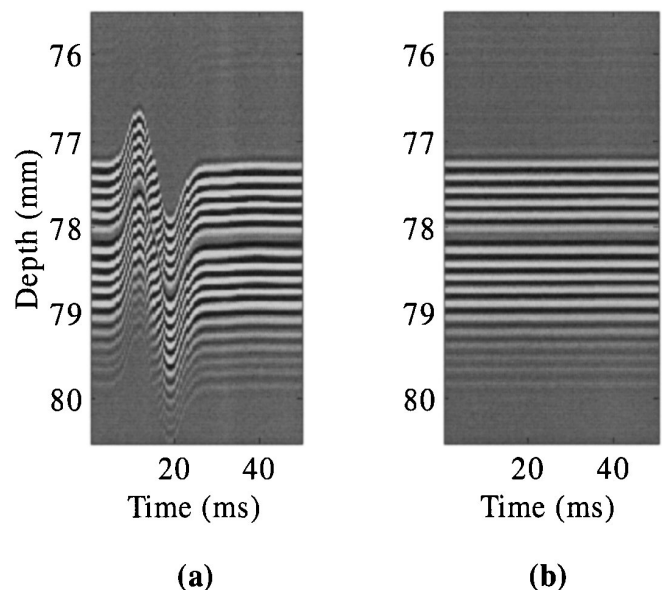


Fig. 10. a) Part of the M-mode image obtained in reflection mode that shows the relative displacement of the lower interface strong echo at $Z = 78$ mm. The RF lines are shifted back with respect to this displacement that corresponds to the opposite of the vibrator absolute displacement. The strong echo is motionless in the M-mode image obtained after compensation (b).

TABLE I
SHEAR VELOCITY AND SHEAR MODULUS ESTIMATES. COMPARISON BETWEEN THE TRANSMIT AND REFLECTION MODES.

	Transmit mode	Reflection modes		
		MIRD	MDEA	SA
Shear velocity (m/s)	1.54 ± 0.02	1.51 ± 0.02	1.72 ± 0.04	1.54 ± 0.02
Shear modulus (kPa)	2.36 ± 0.05	2.28 ± 0.04	2.96 ± 0.14	2.36 ± 0.04

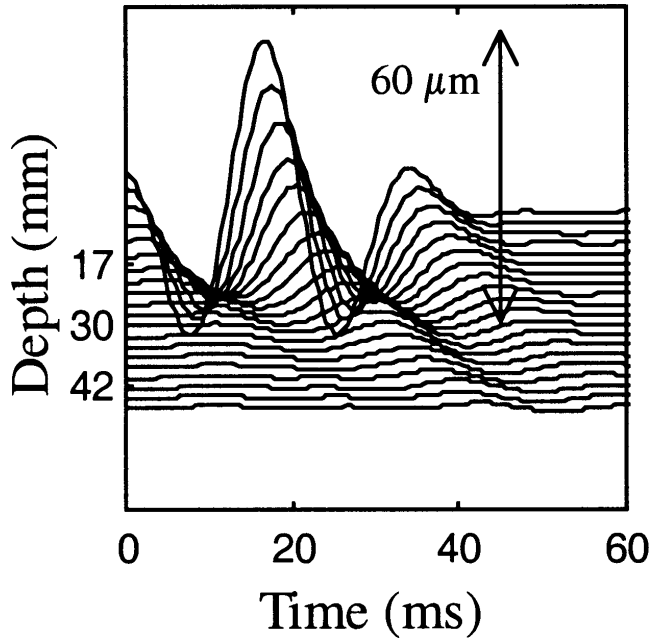


Fig. 11. Displacement estimates measured in the phantom after compensation of the relative displacement of the vibrator deduced from the relative displacement of the strong echo coming from the lower interface of the medium.

C. Discussion

Table I summarizes the different estimates of the shear velocities and shear moduli in the phantom using the transmit and reflection modes. Given the mass density, shear moduli can be obtained using (3). The mass density of our phantoms is about the same as water: $1000 \text{ kg} \times \text{m}^{-3}$. Although no comparison has been carried out with other elasticity estimation techniques, the values indicated in the table seem reasonable. The shear velocity reference estimate is obtained in transmit mode: $1.54 \pm 0.02 \text{ m/s}$. In reflection modes, the shear velocity estimates are in good agreement, whatever the technique, because the variations, compared with the reference, are inferior to 12%. The MDEA mode induces the largest error on the shear velocity estimation because the vibrator displacement compensation is incorrect. The error is small (2%) with the MIRD mode and very small with the SA mode. The strain approach perfectly compensates the transducer relative displacement. It yields to the same shear velocity and shear modulus estimates as in transmit mode.

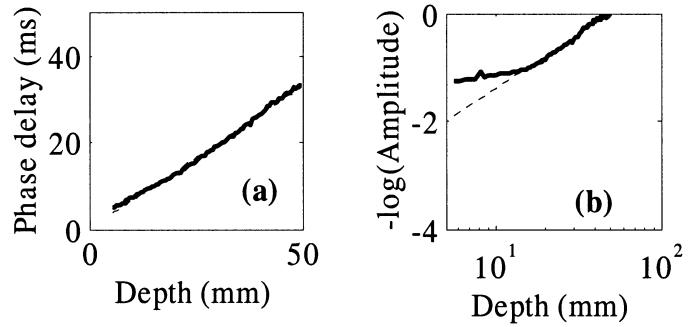


Fig. 12. Reflection mode (MIRD). Phase delay (a) and amplitude (b) of the shear wave as a function of depth after compensation of the relative displacement of the vibrator. A linear fit indicates a shear phase velocity at 50 Hz of $1.51 \pm 0.02 \text{ m/s}$.

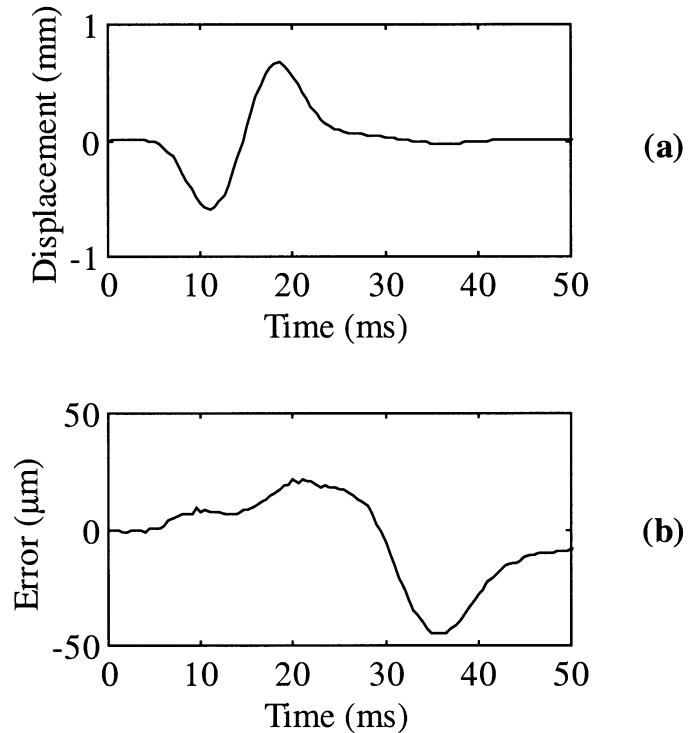


Fig. 13. a) Vibrator displacement estimates deduced from the relative displacement of the echo at $Z = 50 \text{ mm}$. b) Error obtained by comparison with the exact displacement.

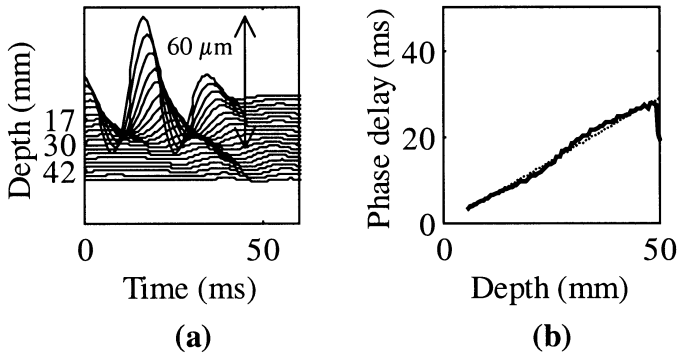


Fig. 14. Reflection mode (MDEA). Displacement estimates (a) and phase delay (b) of the shear wave as a function of depth after compensation of the relative displacement of the vibrator. A linear fit indicates a shear phase velocity at 50 Hz of 1.72 ± 0.04 m/s.

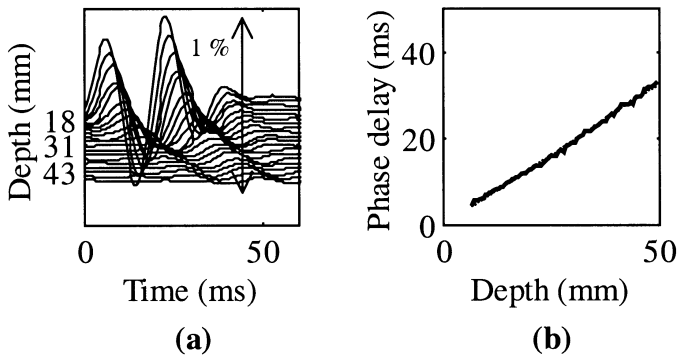


Fig. 15. Reflection mode (SA). Strain estimates (a) and phase delay (b) of the shear wave as a function of depth after compensation of the relative displacement of the vibrator. A linear fit indicates a shear phase velocity at 50 Hz of 1.54 ± 0.02 m/s.

IV. IN VIVO EXPERIMENTS

As far as the in vivo experiments on the human biceps are concerned, the motion compensation technique, perfectly adapted, is the MIRD mode. Indeed, the motionless reference is given by the echo of the humerus bone. This latter hypothesis is quite justified because the insonification time (80 ms) is much smaller than any natural motion of the humerus bone. The following experiment is achieved. A subject is loaded with 1.5-kg weights up to 9 kg then unloaded. A whole experiment lasts 1 min, and the signals are analyzed afterward. An error bar on the velocity is the standard deviation of the linear fit operated on the experimental phase of the shear wave. Fig. 17 shows that the velocity is increased up to a factor of 4 during the contraction of the muscle. It represents, in a simple elastic model, a factor of 16 on the Young modulus. In addition, the velocity during the unloading remains higher than during the loading. This observation could be related to the fatigue of the muscle. Thus, a potential application in the treatment of muscle diseases such as myopathy is hopeful.

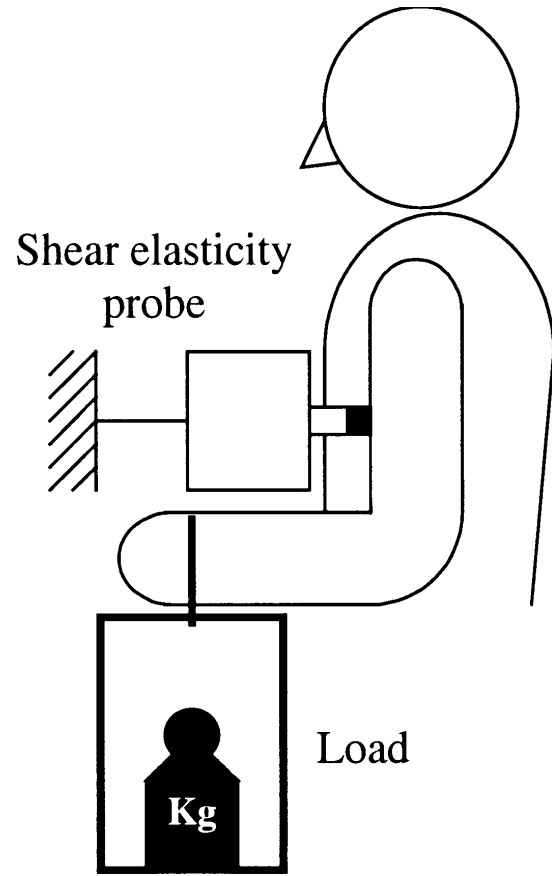


Fig. 16. Experimental setup for in vivo measurements.

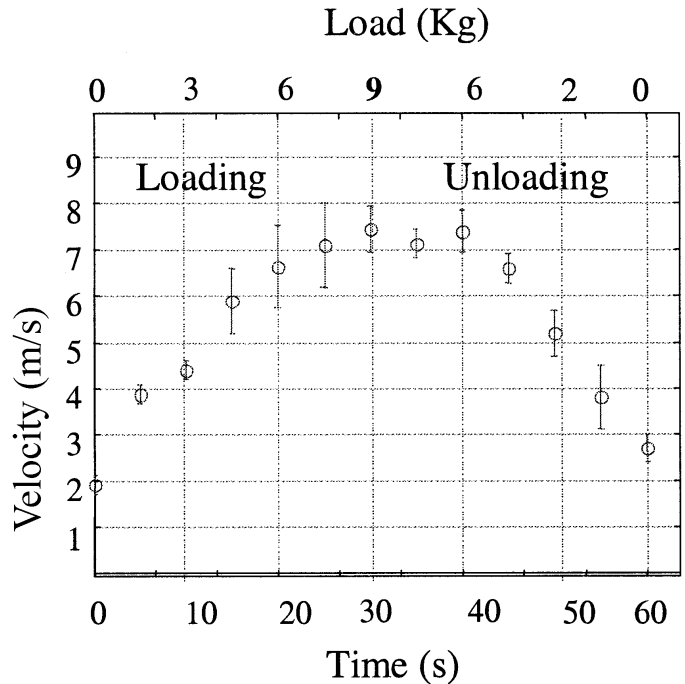


Fig. 17. Velocity of the shear wave in a human bicep contracted by various loads.

V. CONCLUSION

In transient elastography, the transmit mode can be used to measure the shear modulus or shear velocity in soft tissues. This mode suffers from a major drawback because it requires access to both sides of the medium. Thus, we developed the reflection mode that needs only access to one side of the medium. This second mode is validated through careful comparison with the transmit mode.

Based on the reflection mode, the shear elasticity probe is a portable device that could be useful to evaluate the shear modulus or Young Modulus of soft tissues with numerous potential applications in medicine and in the food industry. For medical applications, the crucial point is that the technique is non-invasive, instantaneous, and does not carry any side effects. The shear elasticity probe can also be used to mechanically scan the medium and construct a 2-D or even 3-D map of the Young's modulus.

ACKNOWLEDGMENTS

We would like to thank Isabelle M  nier, Michel Parise, and Jean-Michel Hasquenoph for their expert assistance.

REFERENCES

- [1] S. Catheline, F. Wu, and M. Fink, "A solution to diffraction biases in sonoelasticity: The acoustic impulse technique," *J. Acoust. Soc. Amer.*, vol. 105, no. 5, pp. 2941–2950, 1999.
- [2] S. Catheline, J. L. Thomas, F. Wu, and M. Fink, "Diffraction field of a low-frequency vibrator in soft tissues using transient elastography," *IEEE Trans. Ultrason., Ferroelect., Freq. Contr.*, vol. 46, no. 4, pp. 1013–1020, 1999.
- [3] X. T. Truong, "Extensional wave-propagation characteristics in striated muscle," *J. Acoust. Soc. Amer.*, vol. 51, pp. 1352–1356, Mar. 1971.
- [4] —, "Viscoelastic wave propagation and rheologic properties of skeletal muscle," *Amer. J. Physiol.*, vol. 226, pp. 256–264, Feb. 1974.
- [5] T. A. Krouskop, B. S. Dougherty, and F. S. Vinson, "A pulsed Doppler ultrasonic system for making noninvasive measurements of the mechanical properties of soft tissue," *J. Rehabil. Res. Dev.*, vol. 24, pp. 1–8, 1987.
- [6] R. M. Lerner, S. R. Huang, and K. J. Parker, "'Sonoelasticity' images derived from ultrasound signals in mechanically vibrated tissues," *Ultrasound Med. Biol.*, vol. 16, no. 3, pp. 231–239, 1990.
- [7] K. J. Parker, S. R. Huang, and R. M. Lerner, "Tissue response to mechanical vibrations for 'sonoelasticity imaging'," *Ultrasound Med. Biol.*, vol. 16, no. 3, pp. 241–246, 1990.
- [8] F. Lee, J. P. Bronson, R. M. Lerner, K. J. Parker, S. R. Huang, and D. J. Roach, "Sonoelasticity imaging: Results in vitro tissue specimens," *Radiology*, pp. 237–239, 1991.
- [9] L. Gao, K. J. Parker, R. M. Lerner, and S. F. Levinson, "Imaging of the elastic properties of tissue—A review," *Ultrasound Med. Biol.*, vol. 22, no. 8, pp. 959–977, 1996.
- [10] Y. Yamakoshi, J. Sato, and T. Sato, "Ultrasonic imaging of internal vibration of soft tissue under forced vibration," *IEEE Trans. Ultrason., Ferroelect., Freq. Contr.*, vol. 37, no. 2, pp. 45–53, 1990.
- [11] J. Ophir, E. I. Cespedes, H. Ponnekanti, Y. Yazdi, and X. Li, "Elastography: A method for imaging the elasticity in biological tissues," *Ultrason. Imaging*, vol. 13, pp. 111–134, 1991.
- [12] J. Ophir, E. I. Cespedes, B. Garra, H. Ponnekanti, Y. Huang, and N. Maklad, "Elastography: Ultrasonic imaging of tissue strain and elastic modulus *in vivo*," *Eur. J. Ultrasound*, vol. 3, pp. 49–70, 1996.
- [13] J. Ophir, F. Kallel, T. Varghese, M. Bertrand, E. I. Cespedes, and H. Ponnekanti, "Elastography: A system approach," *Intern. J. Imag. Systems Tech.*, vol. 8, pp. 89–103, 1997.
- [14] R. Muthupillai, D. J. Lomas, P. J. Rossman, J. F. Greenleaf, A. Manduca, and R. L. Ehman, "Magnetic resonance elastography by direct visualization of propagating acoustic strain waves," *Science*, vol. 269, pp. 1854–1857, 1995.
- [15] V. Dutt, R. R. Kinnick, and J. F. Greenleaf, "Acoustic shear wave displacement measurement using ultrasound," in *Proc. IEEE Ultrason. Symp.*, vol. 2, pp. 1185–1193, 1996.
- [16] S. F. Levinson, M. Shinagawa, and T. Sato, "Sonoelastic determination of human skeletal muscle elasticity," *J. Biomech.*, vol. 28, no. 10, pp. 1145–1154, 1995.
- [17] L. Sandrin, S. Catheline, M. Tanter, X. Hennequin, and M. Fink, "Time-resolved pulsed elastography," *Ultrason. Imaging*, vol. 21, pp. 259–272, 1999.
- [18] L. Sandrin, M. Tanter, S. Catheline, and M. Fink, "Shear modulus imaging with 2D transient elastography," *IEEE Trans. Ultrason., Ferroelect., Freq. Contr.*, vol. 49, no. 4, Apr. 2002.
- [19] A. P. Sarvazyan, "Biophysical bases of elasticity imaging," *Acoust. Imaging*, vol. 21, pp. 223–240, 1995.
- [20] M. O'Donnell, A. R. Skovoroda, B. M. Shapo, and Y. Emelianov, "Internal displacement and strain imaging using ultrasonic speckle tracking," *IEEE Trans. Ultrason., Ferroelect., Freq. Contr.*, vol. 41, no. 3, pp. 314–325, May 1994.
- [21] J. A. Jensen, *Estimation of Blood Velocities Using Ultrasound*. Cambridge University Press, 1996, ch. 8.
- [22] W. F. Walker and G. E. Trahey, "A fundamental limit on the performance of correlation based on phase correction and flow estimation technique," *IEEE Trans. Ultrason., Ferroelect., Freq. Contr.*, vol. 41, 1994.
- [23] D. Royer and E. Dieulesaint, *Elastic Waves in Solids*, vol. 1, Springer, 2000.
- [24] K. Aki and P. G. Richard, *Quantitative Seismology, Theory and Methods*, vol. 1, San Francisco: W. H. Freeman and Company, 1980, ch. 4.
- [25] S. K. Alam, J. Ophir, and E. E. Konofagou, "An adaptive strain estimator for elastography," *IEEE Trans. Ultrason., Ferroelect., Freq. Contr.*, vol. 45, no. 2, pp. 461–472, Mar. 1998.



Laurent Sandrin was born in Massy, France on March 21, 1973. He received an Ing. degree from the Ecole Sup  rieure de Physique et de Chimie Industrielles de la Ville de Paris (ESPCI) with a specialization in physics in 1996. In 1994, he worked at the Sony Research Center in Yokohama, Japan on large band-gap semiconductors for blue laser diodes. In 1996, he joined the G  nie Physique Department of the Ecole Polytechnique de Montr  al (Canada) to study the adhesion between meals (Al, Cu) and polymer films (PE, PET).

In 2000, he received the Ph.D. at the Laboratoire Ondes & Acoustique in Paris, where he works on elastography as well as ultrafast imaging under the supervision of Mathias Fink.



Micka  l Tanter was born in December 1970 in Paimpol, France. He received the engineer degree in electronics of SUPELEC in 1994 and the Ph.D. in acoustics at the University of Paris VII in 1999. He is now a researcher in the National French Center of Science (C.N.R.S.). His current research interests include focusing techniques in heterogeneous media, medical ultrasonic imaging (such as ultrasonic brain imaging and elastography), ultrasonic therapy, and nonlinear acoustics.

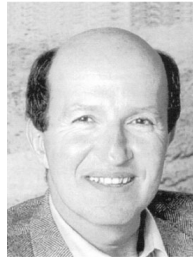


Jean-Luc Gennisson was born in 1974 in Paris, France. He received the D.E.A. degree in electronics from Paris VI University in 2000. He is currently working toward his Ph.D. from Paris VI University on time-resolved I-D pulsed elastography.



Stefan Catheline was born in 1970 in Ghardaia, Algeria. He received the DEA degree in acoustic physics in 1994 from Paris VI University, France. In 1998, he received his Ph.D. degree in physics from Paris VII (Denis Diderot) for his work on transient elastography. After a post doc at Scripps Institution of Oceanography, Marine Physical Laboratory, he became an assistant professor at Paris VII University in 1999 and joined the Laboratory Ondes et Acoustique at the Ecole Supérieur de Physique et de Chimie Industrielle de la

ville de Paris (ESPCI). His current research activities include shear waves in soft tissues and dynamic focusing using time reversal process in wave guides.



Mathias A. Fink received the diplome de Doctorat de 3^{ème} cycle in solid state physics in 1970 and the Doctorat ès-Sciences degree in acoustics in 1978 from Paris University, France.

From 1981 to 1984, he was a professor of acoustics at Strasbourg University, France. Since 1984, he has been a professor of physics at Paris University (Denis Diderot), France. In 1990, he founded the Laboratoire Ondes et Acoustique at the Ecole Supérieure de Physique et de Chimie Industrielles de la Ville de Paris (ESPCI). In 1994, he was elected at the Institut Universitaire de France.

His current research interests include medical ultrasonic imaging, ultrasonic therapy, nondestructive testing, underwater acoustics, active control of sound and vibration, analogies between optics and acoustics, wave coherence in multiple scattering media, and time reversal in physics. He has developed different techniques in speckle reduction, wave focusing in inhomogeneous media, and ultrasonic laser generation. He holds 20 patents, and he has published more than 220 articles.